Available online at www.sciencedirect.com
ScienceDirect
Trans. Nonferrous Met. Soc. China 27(2017) 2443−2453
Transactions of Nonferrous Metals Society of China
www.tnmsc.cn

Tensile stress−strain behavior of metallic alloys

Jun CAO, Fu-guo LI, Xin-kai MA, Zhan-kun SUN

State Key Laboratory of Solidification Processing, School of Materials Science and Engineering,
Northwestern Polytechnical University, Xi'an 710072, China

Received 1 July 2016; accepted 17 March 2017

Abstract: Tensile stress−strain curves of five metallic alloys, i.e., SKH51, STS316L, Ti−6Al−4V, Al6061 and Inconel600 were analyzed to investigate the working hardening behavior. The constitutive parameters of three constitutive equations, i.e., the Hollomon, Swift and Voce equations, were compared by using different methods. A new working hardening parameter was proposed to characterize the working hardening behavior in different deformation stages. It is found that Voce equation is suitable to describe stress−strain curves in large strain region. Meanwhile, the predicting accuracy of ultimate tensile strength by Voce equation is the best. The working hardening behavior of SKH51 is different from the other four metallic alloys.

Key words: constitutive equation; tensile stress−strain behavior; piecewise fitting; coordinate transformation

1 Introduction

It is significant to predict plastic deformation in describing stress−stain curve by using constitutive equation. Furthermore, applying appropriate constitutive equation is especially important to predict tensile properties and to access structural integrity during service [1]. Classical constitutive equations include Hollomon [2], Voce [3], Ludwigson [4] equations and so on. More recently, a "H/V" hardening model [5] was introduced, which combined Hollomon and Voce forms by a linear weight temperature-dependent factor. Many researchers [6−9] took strain rate and temperature into account to study constitutive equations of metallic alloys. Power-law type constitutive equations are more suitable for describing tensile stress−strain curves of body-centered cubic (BCC) metals [5]. Exponential-type constitutive equations are suitable for describing tensile stress−strain curves of most face centered cubic (FCC) metals at room temperature [10]. All classical constitutive equations failed to describe working hardening behavior accurately in two distinct stages, and then a piecewise Ramberg−Osgood equation was proposed [11]. SAMUEL [12] revealed the limitations of Hollomon and Ludwigson equations in assessing strain hardening parameters of stainless steel, aluminum, pure nickel, etc. SAINATH et al [13] studied the applicability of Voce equation in describing tensile working hardening behavior of P92. As the characteristics of working hardening behavior vary during plastic deformation of some materials, empirical and phenomenological constitutive equations may not describe stress−strain curves well.

Efforts were made to study the nature of working hardening behavior [14,15] in plastic deformation. In the course of plastic deformation of a metal, dislocations always move simultaneously and some of them compete with each other. Therefore, dislocations motion is the physical nature of working hardening. MONTEIRO and REED-HILL [16] investigated the two deformation stages in stress−strain curve of pure titanium, and concluded that the growth of uniform dislocation distribution and cell structure formation are responsible for the two deformation stages, respectively. Due to a more complex post-yield behavior, simplified empirical equations cannot precisely describe the stress−strain curve. However, UGent models can successfully describe it by using piecewise fitting [17]. In plain carbon steels, the *n* value depends only on the interparticle spacing of cementite, which is related to two parameters, the volume fraction and the particle size. Strain hardening

Foundation item: Project (51275414) supported by the National Natural Science Foundation of China; Project (3102015BJ (II) ZS007) supported by the Fundamental Research Funds for the Central Universities, China; Project (130-QP-2015) supported by the Research Fund of the State Key Laboratory of Solidification Processing (NWPU), China
Corresponding author: Fu-guo LI; Tel: +86-29-88474117; Fax: +86-29-88492642; E-mail: fuguolx@nwpu.edu.cn
DOI: 10.1016/S1003-6326(17)60271-1

and softening processes are competitive during the plastic deformation and the generation and annihilation of dislocation happen. Therefore, metallic alloy presents different hardening stages in the working hardening rate−stress curve [18]. A Kocks−Mecking type curve [14] of strain hardening rate versus net flow stress presents different deformation stages for different materials. These stages occurred in Kocks−Mecking type are related to dislocation mobility, cross-slip of dislocations, dynamic recovery and microstructure characteristics [19]. A very convenient method to distinguish deformation stages in the stress−strain curves is the Crussard−Jaoul (CJ) analysis where $d\sigma/d\varepsilon_p$−ε_p data are plotted in lg−lg coordinates. Constitutive parameters play a great role in estimating some mechanical properties, such as yield strength (YS), ultimate tensile strength (UTS) and fracture strain. The exponent n plays a crucial role in sheet metal forming. Therefore, microstructure evolution during work hardening is closely related to the manufacture and application of materials.

It is very important to notice that constitutive equation is crucial to predict the plastic deformation. It can be embedded in the finite element method simulations. Therefore, great attention should be given to the constitutive parameters of working hardening behavior. In this work, different deformation stages were distinguished in three coordinate transformations and then piecewise fitting was applied to investigate the working hardening behavior. In addition, the constitutive parameters of three typical constitutive equations for five metallic alloys were investigated. A new working hardening parameter was applied to compare the working hardening behavior in different deformation stages. Furthermore, the predictive accuracy of YS and UTS by using different methods was discussed.

2 Methods

2.1 Constitutive relations

One of the important empirical equations to characterize stress−strain curves of metallic alloy is Hollomon power law:

$$\sigma = K_H \varepsilon_p^{n_H} \tag{1}$$

where K_H is the strength coefficient and n_H is the strain hardening exponent.

If experimental stress−strain curve follows the Hollomon equation, it can be recognized as a straight line in such two equations [11]:

$$\lg \sigma = \lg K_H + n_H \lg \varepsilon_p \tag{2}$$

$$\lg \theta = \lg(K_H n_H) + (n_H - 1) \lg \varepsilon_p \tag{3}$$

where θ is working hardening rate; n_H and K_H can be determined from slope and intercept of ordinate in Eqs. (2) and (3).

Since a good approximation is only restricted to the area of large plastic strain, the Hollomon equation is too simplistic to describe the full-range behavior of some metals. SWIFT [20] proposed another power-law equation, introducing a parameter ε_0, which accounts for a possible pre-strain:

$$\sigma = K_s (\varepsilon_p + \varepsilon_0)^{n_s} \tag{4}$$

where n_s and K_s are strain hardening exponent and strength coefficient. If experimental stress−strain curve follows the Swift equation, the stress−strain curve in a double logarithmic plot of θ against σ related to "modified C−J analysis" [16] is linear, and it is expressed as

$$\lg \theta = \lg(n_s K_s^{1/n_s}) + (1 - \frac{1}{n_s}) \lg \sigma \tag{5}$$

According to this equation, n_s and K_s can be determined from the slope and intercept. However, ε_0 cannot be obtained from linear fitting of Eq. (5).

Hollomon and swift equations both follow power law, while Voce [3] proposed an exponential relation which is fundamentally different from power-law type models. It is expressed as

$$\sigma = \sigma_0 - \sigma_0 A \exp(-\beta \varepsilon_p) \tag{6}$$

where σ_0 is saturation stress and A, β are material coefficients. In Eq. (6) , the flow curve is deemed as a transient form of the flow stress from some starting value to the saturation value corresponding to some equilibrium structures under a given strain rate and temperature [1]. This equation is applicable to characterize the material that follows a linear relation in a plot of θ−σ referred to Ref. [21]:

$$\theta = \beta(\sigma_0 - \sigma) \tag{7}$$

This equation can determine the coefficients σ_0 and β from the slope and intercept. A cannot be obtained from the linear fitting of this equation. Voce-type models approach a saturation stress at large strain, while power-law models are unsaturated at large strain [2].

The three transformations ($\lg \theta$ vs $\lg \varepsilon_p$, $\lg \theta$ vs $\lg \sigma$ and θ vs σ) are convenient to distinguish the deformation stages. Since some parameters (ε_0 and A) cannot be determined by linear fitting, the original constitutive equations can be used to piecewise fit experimental stress−strain curves. In order to comprehensively evaluate the working hardening behavior for the power-law relations, we define a working hardening parameter χ_P as

$$\chi_P = \frac{\partial \sigma^{1/n}}{\partial \varepsilon_p} = K^{1/n} \tag{8}$$

To predict yield strength (YS) and ultimate tensile strength (UTS), the calculation methods of YS and UTS by three constitutive equations are summarized in Table 1. The calculation methods of YS are based on the definition and the calculation methods of UTS are based on the instability condition:

$$\theta=\sigma \tag{9}$$

Table 2 gives tensile properties of five metallic alloys [22] from true stress−strain curves.

2.2 Fitting methods

Tensile stress strain curves [22] of five metallic alloys, SKH51 (carbon steel), STS316L (austenite-based stainless steel), Ti−6Al−4V (Ti alloy), Al6061 (Al alloy) and Inconel600 (Ni base Superalloy) were analyzed, as shown in Fig. 1. True total strain was transformed into true plastic strain by subtracting elastic strain (σ_t/E). Then, data fitting was processed with least square regression. Fitting data points were chosen from YS to UTS in full range fitting. Additionally, data points of piecewise fitting were chosen from different deformation stages. To obtain reasonable results, the data points in three transformations of lg θ vs lg ε_p, lg θ vs lg σ and θ vs σ were smoothened. The predictive accuracy of YS and UTS by using piecewise fitting and full range fitting were compared respectively.

Table 1 Calculation methods of yield strength and ultimate tensile strength by three constitutive equations

Method	Yield strength	Ultimate tensile strength
Hollomon equation	$\sigma_s=K_H\cdot(0.002)^{n_H}$	$\sigma_u=Kn_H^{n_H}$
Swift equation	$\sigma_s=K_s\varepsilon_0^{n_s}$	$\sigma_u=K(n_s-\varepsilon_0)^{n_s}$
Voce equation	$\sigma_s=\sigma_0-\sigma_0 A$	$\sigma_u=\sigma_0\beta/(1+\beta)$

Table 2 Elastic modulus, yield strength and ultimate tensile strength data for some samples [22]

Sample	Elastic modulus/GPa	YS data		UTS data	
		True strain	Stress/MPa	True strain	Stress/MPa
SKH51 (tempered)	223	0.0033	280	0.1181	785
STS316L (annealed)	198	0.0035	305	0.4524	949
Ti−6Al−4V (solution-treated)	110	0.0104	930	0.0858	1097
Al6061 (solution-treated)	70	0.0057	259	0.0508	298
Inconel600 (annealed)	170	0.0044	405	0.2715	985

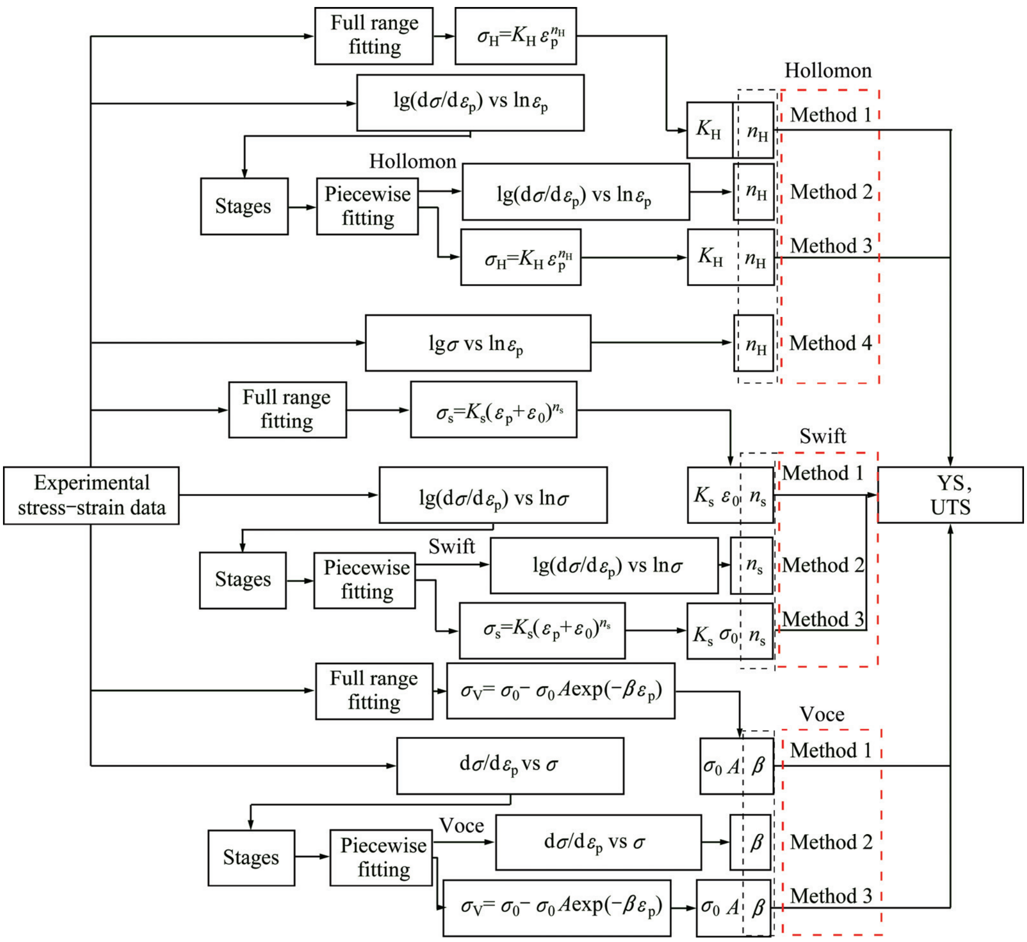

Fig. 1 Outline of different fitting methods for experimental stress−strain data

In the piecewise fitting, constitutive parameters were obtained by original equations rather than linear equations. The reason is that predictive accuracy of the constitutive parameters from linear fitting is less accurate than that fitted by original equation. Generally, constitutive parameters fitted in deformation stage I and final deformation stage were used to predict YS and UTS, respectively. In addition, in order to make discontinuous points transform into continuous points in the piecewise fitting, a weighted fitting was used. Experimental data were analyzed by applying the commercial software Origin Pro 8.0 SRO (Origin Lab Co., MA). Table 3 gives all constitutive parameters and predictive accuracy by Hollomon, Swift and Voce equations with piecewise fitting and full range fitting.

3 Results and discussion

3.1 Analysis of deformation stages for metallic alloys

Figure 2(a) presents true stress−true plastic strain curve of SKH51 and the linear fitting result for data points of lg σ vs lg ε_p. The stress−strain curve shows power law type strain hardening without turning point. It can be observed that two deformation stages occur in the transformation of lg θ vs lg ε_p (Fig. 2(b)), and three deformation stages exist in other two transformations of lg θ vs lg σ (Fig. 2(c)) and θ vs σ (Fig. 2(d)). In addition, there are some differences between the transition regions in the two transformations (lg θ vs lg σ and θ vs σ). This indicates that the working hardening behavior is different under different scales. In carbon steel, the interparticle spacing of cementite is considered as the mean free path (MFP) of dislocation motion, and the n value of metals is proportional to the MFP [23]. Sensitivity to stress and strain of materials is the reason that different deformation stages occur in different coordinate transformations.

Figure 3(a) presents true stress−true plastic strain curve of STS316L and the linear fitting result for data points of lg σ vs lg ε_p. The true stress−true plastic strain curve of STS316L shows linear-type strain hardening and it presents obvious working hardening behavior. It can be observed that three deformation stages occur in the transformation of lg θ vs lg ε_p (Fig. 3(b)), while two deformation stages exist in other two transformations lg θ vs lg σ (Fig. 3(c)) and θ vs σ (Fig. 3(d)). In addition, there are small differences between transition regions in the two transformations (lg θ vs lg σ and θ vs σ), which are different from the transitions in the transformation of lg θ vs lg ε_p. This indicates that the working hardening mechanisms reflected by the two transformations of lg θ vs lg σ and θ vs σ are the same. The transformation from planar slip to cross slip systems and dynamic recovery is the reason why stages occur in related coordinate systems [12].

Table 3 Constitutive parameters in Hollomon, Swift and Voce equations fitted to stress−strain points with piecewise fitting and full range fitting by using original equation

Sample	Stage	Hollomon			Swift				Voce			
		n_H	K_H/MPa	R	n_s	K_s/MPa	ε_0	R	σ_0	σ_0*A	β	R
SKH51	I	0.312	1977	0.9992	0.316	1992	0.00013	0.9997	497	335	214	0.997
	II	0.216	1307	0.9885	0.139	1089	−0.00961	0.9999	701	438	63.4	0.9999
	III	−	−	−	0.0977	995	−0.0232	0.9998	816	336	20.9	0.9999
	Full	0.230	1361	0.9778	0.204	1275	−0.0016	0.9892	760	487	47.2	0.9913
STS316L	I	0.064	474	0.9774	0.090	520	0.00143	0.998	363	71	157	0.9937
	II	0.204	830	0.9965	0.5371	1352	0.0699	0.9999	1359	1030	2.02	0.9998
	III	0.390	1276	0.998	−	−	−	−	−	−	−	−
	Full	0.333	1185	0.9552	0.524	1348	0.0636	0.9998	1365	1035	2	0.9991
Ti−6Al−4V	I	0.00726	981	0.9939	0.0271	1089	0.00185	0.9932	957	38.8	356	0.991
	II	0.0324	1138	0.9935	0.0939	1381	0.0137	0.9999	1122	195	24.9	0.9999
	III	0.0641	1291	0.9996	0.0612	1282	−0.00049	0.9998	−	−	−	−
	Full	0.0519	1239	0.9653	0.0839	1347	0.0107	0.999	1123	194	24.7	0.9996
Al6061	I	0.0321	314	0.9996	0.0343	318	6.00E-05	0.9996	261	25	977	0.9981
	II	0.0487	343	0.9995	0.0686	367	0.00373	0.9998	303	49.4	49.8	0.9989
	III	0.062	362	0.9993	−	−	−	−	−	−	−	−
	Full	0.0505	347	0.9813	0.0738	372	0.0054	0.9985	306	49	41.5	0.9984
Inconel600	I	0.0399	539	0.8846	0.0822	643	0.00154	0.9985	441	63.3	282	0.9955
	II	0.244	1297	0.9915	0.458	1738	0.0405	0.9999	1240	832	4.50	0.9999
	III	0.339	1554	0.9987	0.148	1310	−0.12	0.9995	−	−	−	−
	Full	0.264	1351	0.9553	0.427	1670	0.0348	0.9995	1245	836	4.45	0.9997

Deformation stages 1, 2 and 3 represent piecewise fitting using original equations in different deformation stages observed from related coordinate transformations; 'Full' represents full range fitting with typical original equations

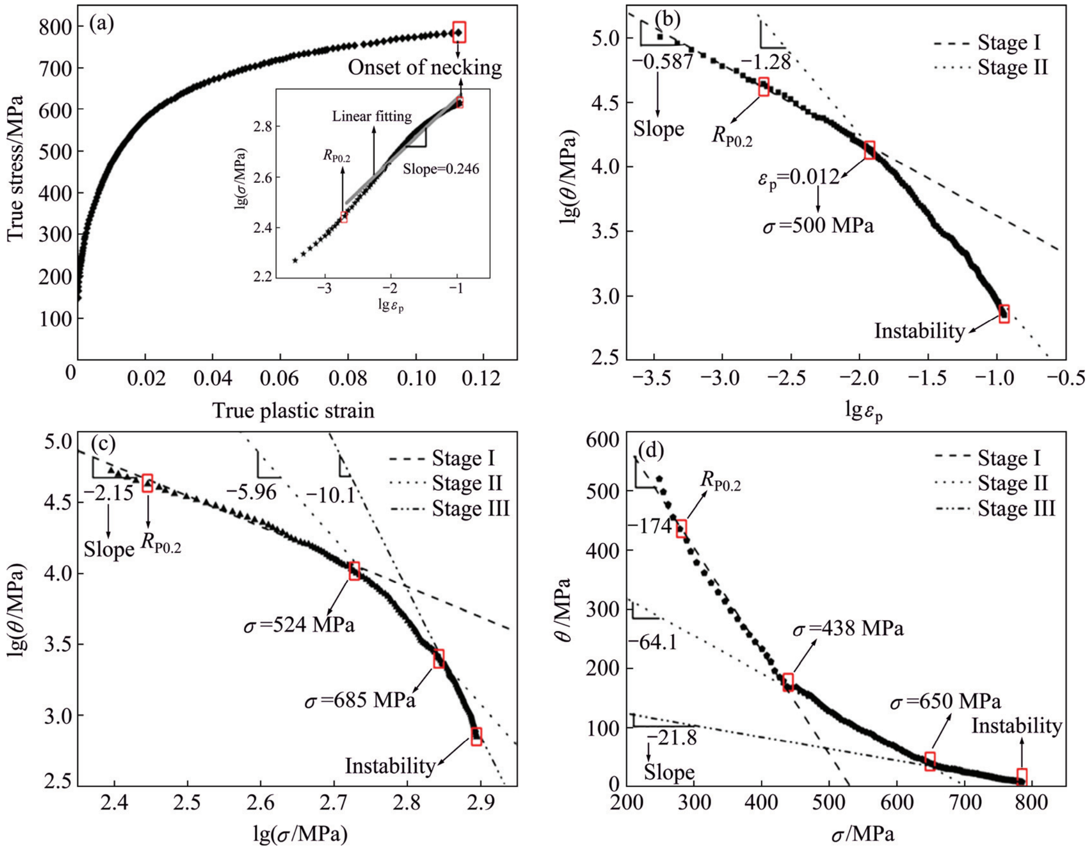

Fig. 2 True stress−strain curve and linear fitting in lg σ vs lg ε_p transformation (a), and deformation stages in lg θ vs lg ε_p (b), lg θ vs lg σ (c) and θ vs σ (d) transformations for SKH51

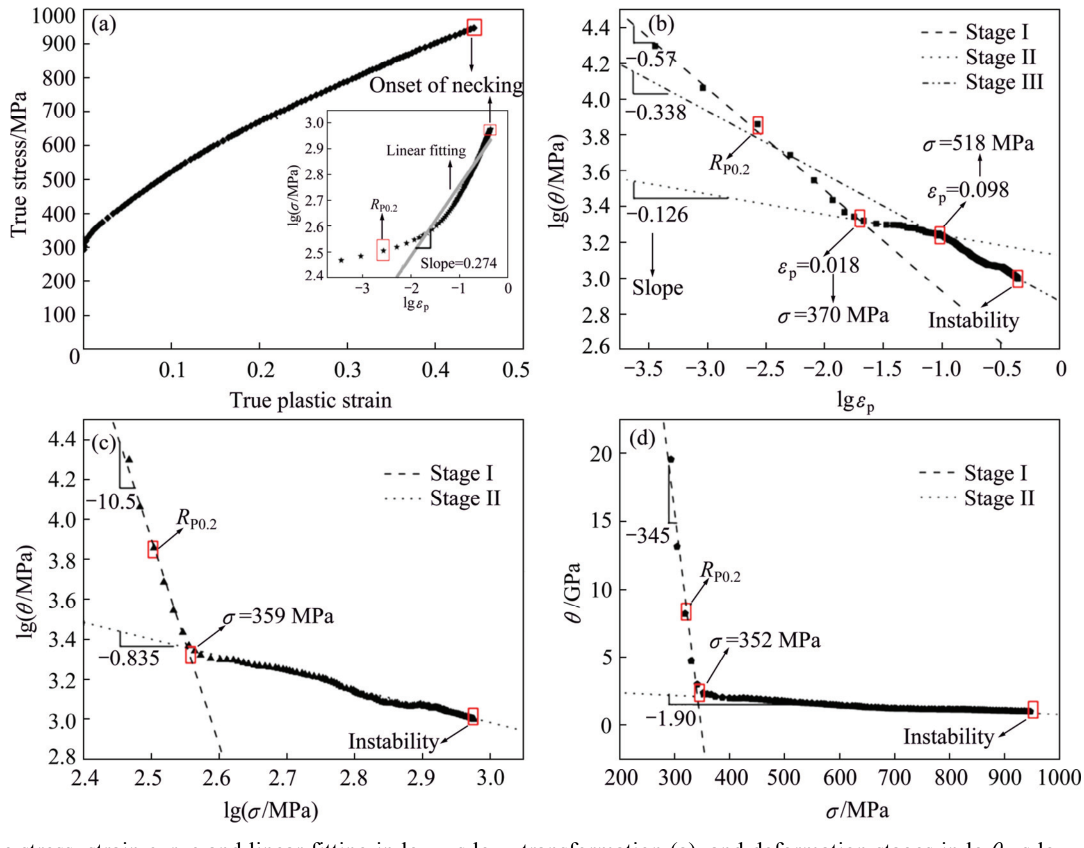

Fig. 3 True stress−strain curve and linear fitting in lg σ vs lg ε_p transformation (a), and deformation stages in lg θ vs lg ε_p (b), lg θ vs lg σ (c) and θ vs σ (d) transformations for STS316L

Figure 4(a) presents true stress−true plastic strain curve of Ti−6Al−4V and the linear fitting result for data points of lg σ vs lg ε_p. The YS is higher, while its working hardening behavior is not significant. The reason is Ti alloys are hard-deformation materials, as shown in Fig. 4(a). It can be observed that three deformation stages occur in the two transformations of lg θ vs lg ε_p (Fig. 4(b)) and lg θ vs lg σ (Fig. 4(c)), while two deformation stages exist in the transformation of θ vs σ (Fig. 4(d)). The deformation stages in the transformation of θ vs σ are different from the deformation stages in the two transformations (lg θ vs lg ε_p and lg θ vs lg σ). This indicates that the applicability of Voce equation is different from the other two equations. The uniform dislocation multiplication and the formation of cell structure are the reasons why stages exist in corresponding coordinate transformations for pure titanium [16]. In addition, the growth of grain size is an important factor in strain hardening for Ti−6Al−4V [24].

Figure 5(a) presents true stress−true plastic strain curve of Al6061 and the linear fitting result for data points of lg σ vs lg ε_p. The true stress−true plastic strain curve (Fig. 5(a)) of Al6061 also presents linear-type strain hardening. It can be observed that three deformation stages occur in the transformation of lg θ vs lg ε_p (Fig. 5(b)), and two deformation stages exist in the two transformations of lg θ vs lg σ (Fig. 5(c)) and θ vs σ (Fig. 5(d)). It is similar to the deformation stages of STS316L. Annihilation and generation of the dislocation are related to the deformation stages of aluminum alloys [25].

Figure 6(a) presents true stress−true plastic strain curve of Inconel600 and the linear fitting result for data points of lg σ vs lg ε_p. The stress−strain curve exhibits obvious working hardening behavior and large plasticity. It can be observed that three deformation stages occur in the deformation stages of lg θ vs lg ε_p (Fig. 6(b)) and lg θ vs lg σ (Fig. 6(c)). In addition, two deformation stages exist in θ vs σ (Fig. 6(d)). The situation of deformation stages is similar to the deformation stages of Ti−6Al−4V. The difference between deformation stages is also related to dislocation mechanism, and the decrease of strain hardening index with stress is a result of dynamic recovery [26].

From the deformation stages in three coordinate transformations for five metallic alloys, it can be observed that the deformation stages of SKH51 are different from the other four metallic alloys. The difference of physical mechanism between two transformations (lg θ vs lg ε_p and lg θ vs lg σ) is the sensitivity of stress and plastic strain to work hardening behavior. In this case, experimental stress−strain data are

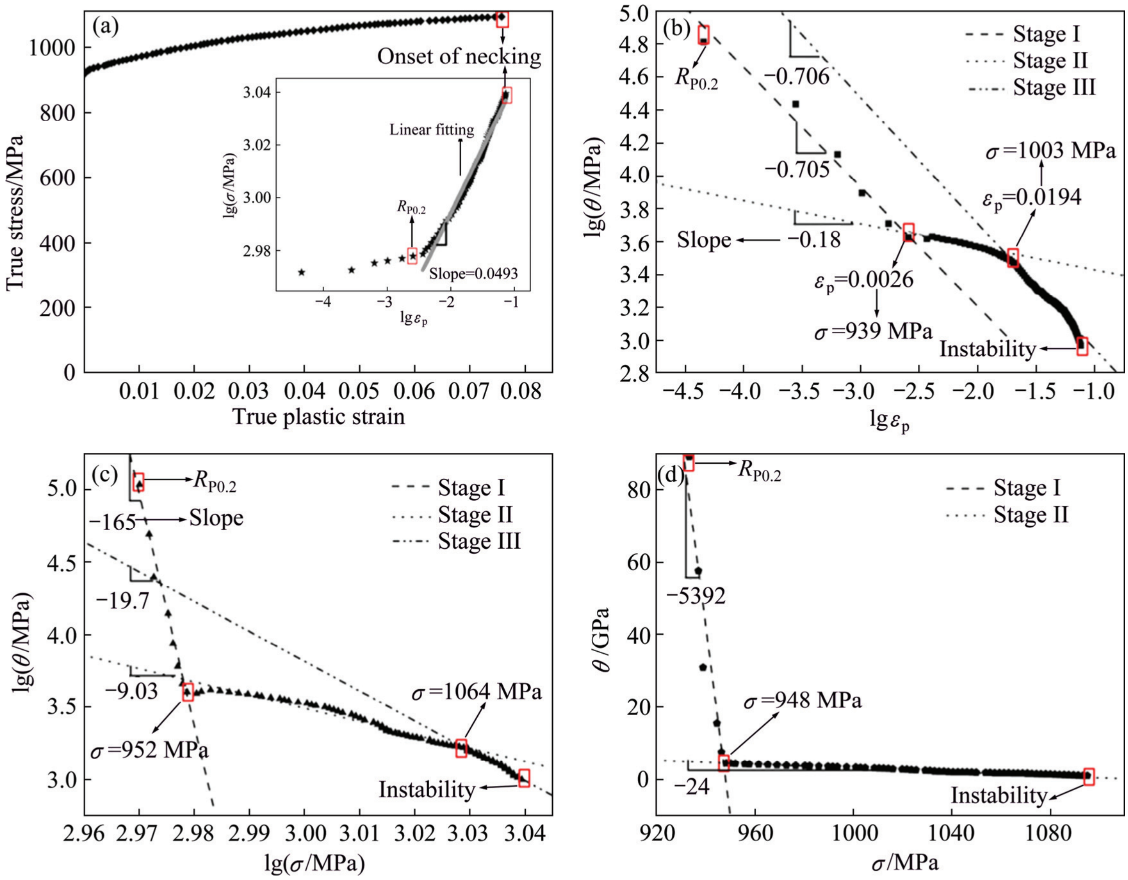

Fig. 4 True stress−strain curve and linear fitting in lg σ vs lg ε_p transformation (a), and deformation stages in lg θ vs lg ε_p (b), lg θ vs lg σ (c) and θ vs σ (d) transformations for Ti−6Al−4V

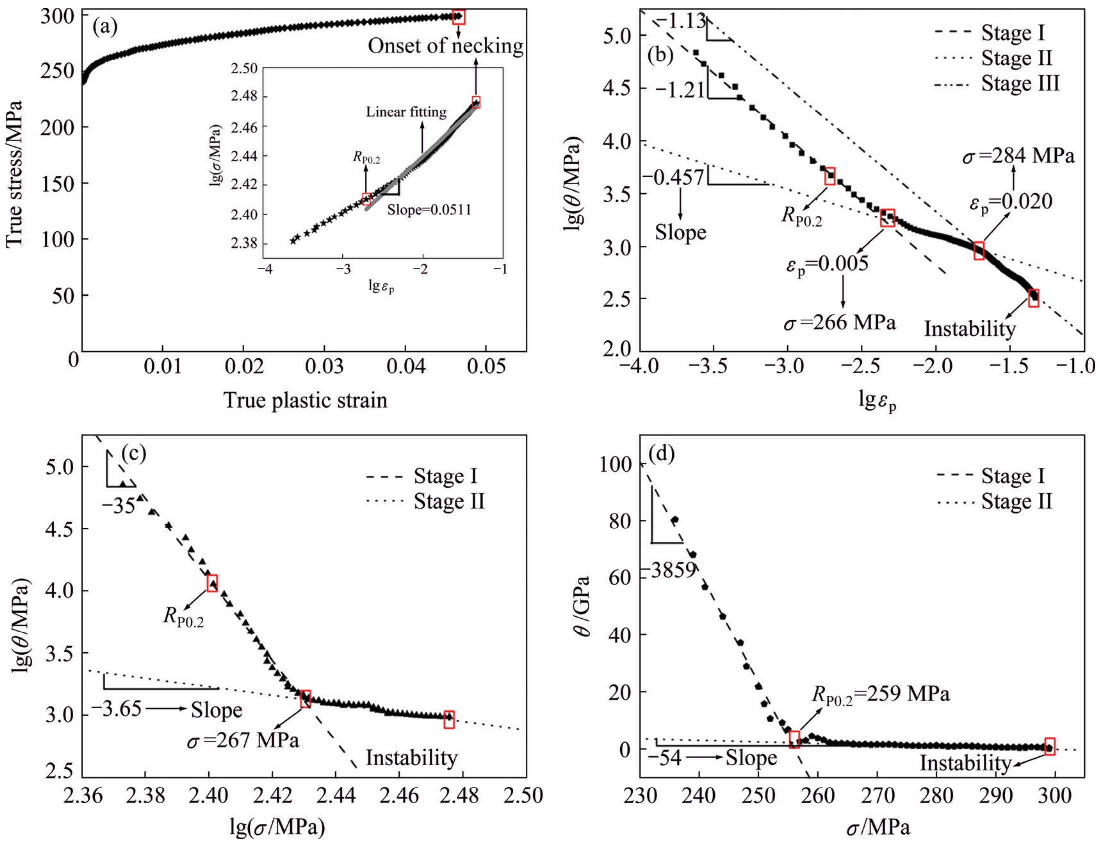

Fig. 5 True stress−strain curve and linear fitting in lg σ vs lg ε_p transformation (a), and deformation stages in lg θ vs lg ε_p (b), lg θ vs lg σ (c) and θ vs σ (d) transformations for Al6061

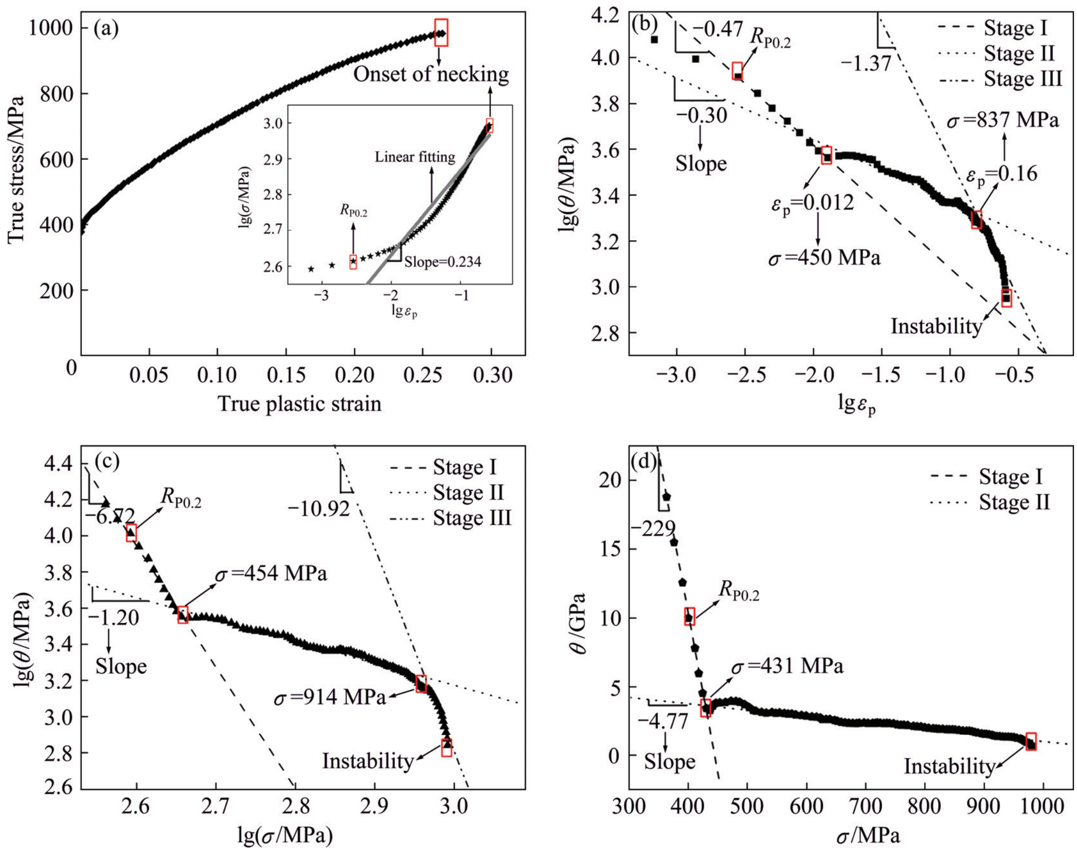

Fig. 6 True stress−strain curve and linear fitting in lg σ vs lg ε_p transformation (a), and deformation stages in lg θ vs lg ε_p (b), lg θ vs lg σ (c) and θ vs σ (d) transformations for Inconel600

converted into two transformations and the deformation stages may be different.

On the other hand, the difference between two transformations ($\lg\theta$ vs $\lg\sigma$ and θ vs σ) is that the former is conducted by a logarithm analysis. Even if there is no significant deformation stage in the coordinate transformation of θ vs σ, the deformation stages may exist in the transformation of $\lg\theta$ vs $\lg\sigma$. The linear fitting conditions of the three coordinate transformations ($\lg\theta$ vs $\lg\varepsilon_p$, $\lg\theta$ vs $\lg\sigma$ and θ vs σ) reflect that the applicability of constitutive equations in low and large strain regions may be different. As noted in Table 3, it is found that Swift equation is the most suitable to describe the stress−strain curves in low strain region and Voce equation is the most suitable to describe the stress−strain curves in large strain region.

3.2 Constitutive parameters

As can be observed in Fig. 7, constitutive parameters (n_H, n_s and β) of three typical constitutive

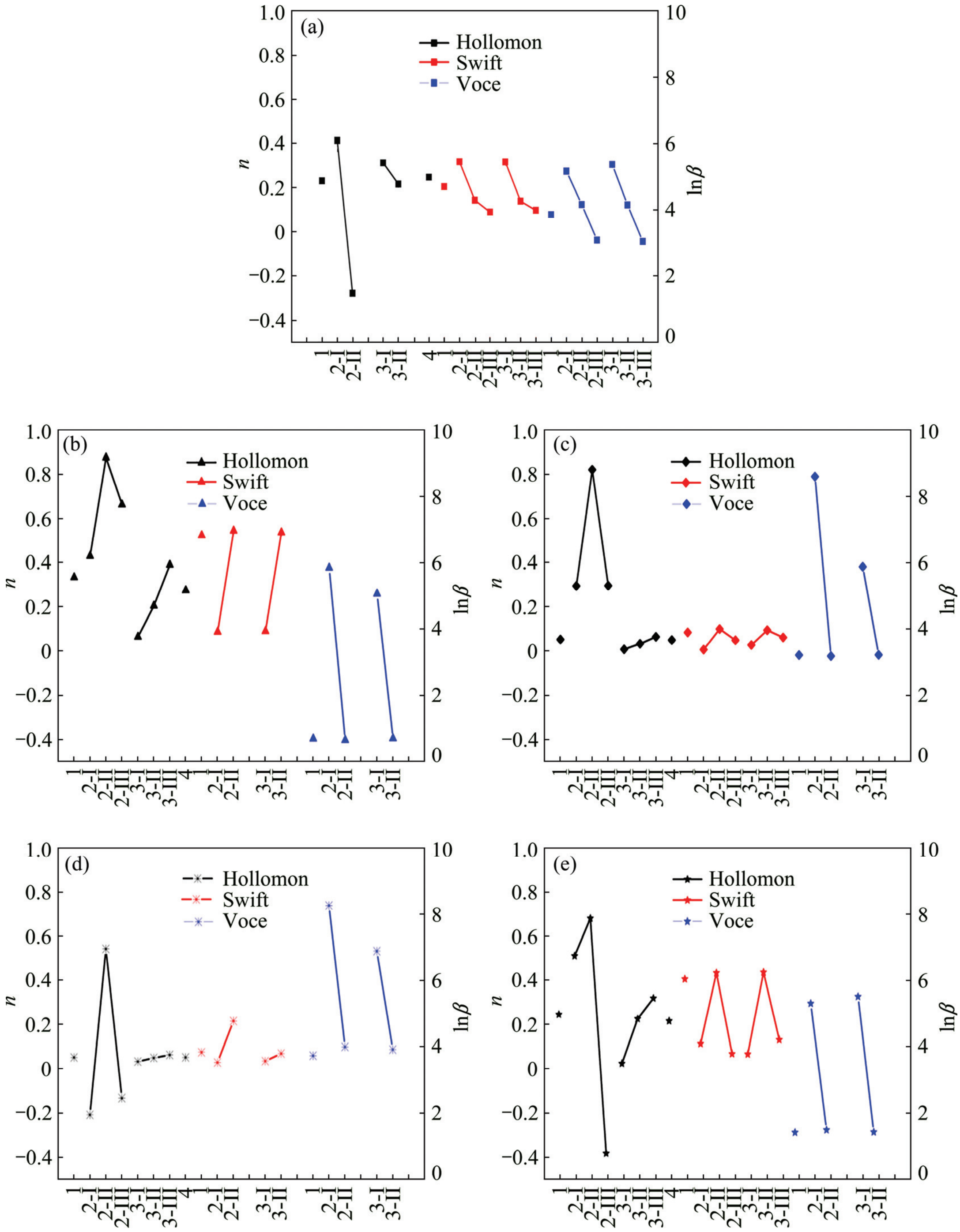

Fig. 7 Comparisons of constitutive parameters in three constitutive equations with different methods: (a) SKH51; (b) STS316L; (c) Ti−6Al−4V; (d) Al6061; (e) Inconel600 (Number (1, 2, 3 and 4) represent different methods, as shown in Fig. 1; I, II and III represent different deformation stages)

equations were compared by different methods for five metallic alloys. For the analysis of n_H, there are two methods, one of which is full range fitting by Hollomon equation and the other is full range fitting of the data points on $\lg\theta$ vs $\lg\varepsilon_p$. The difference between two methods is small for five metallic alloys. n_H determined by fitting the data points on $\lg\theta$ vs $\lg\varepsilon_p$ in different deformation stages is changed a lot. However, n_H determined by fitting original constitutive equations is gradually changed and it shows small difference from the previous two full range fitting methods. n_H decreases in the different deformation stages of SKH51 by original equations, and it increases for the other four metallic alloys. This indicates that the working hardening behavior of SKH51 is different from the other four metallic alloys. n_H fitted by full range fitting is equal to the average of all parameters by piecewise fitting in deformation stages. However, it is meaningful to obtain strain hardening index in all stages for guiding sheet metal forming.

For the analysis of n_s, the difference between piecewise fitting with linear equation and original equation is small. The downward trend of n_s for SKH51 is different from the other four metallic alloys. The reason is that working hardening behavior of carbon steel is different from other alloys. In order to evaluate the constitutive parameter β, it is transformed to $\ln\beta$ so as to compare with n_H and n_s under the same scale.

For the analysis of $\ln\beta$, the difference between piecewise fitting with linear equation and original equation is small in large strain region. The difference can be observed in final deformation stage for SKH51 and in deformation stage II for the other four metallic alloys. However, the difference is large in deformation stage I. In addition, the difference between full range fitting with original equation and piecewise fitting in final stage is small except for SKH51. This indicates that the difference of fitting by Voce equation between low and large strain region is significant. There are three deformation stages for SKH51 and two deformation stages for other four metallic alloys, and those are also related to strain hardening characteristics of materials. For the different deformation stages in three coordinate transformations ($\lg\theta$ vs $\lg\varepsilon_p$, $\lg\theta$ vs $\lg\sigma$ and θ vs σ), the constitutive parameters of these stages are also different.

Figure 8 shows tendency of working hardening parameters χ_P for five metallic alloys. The constitutive parameters (K and n) were chosen from the piecewise fitting results in different deformation stages of two transformations ($\lg\theta$ vs $\lg\varepsilon_p$ and $\lg\theta$ vs $\lg\sigma$). For different deformation stages in the two transformations, $\ln\chi_P$ was used to comprehensively evaluate the different working hardening behaviors. Figure 8(a) shows that $\ln\chi_P$ exhibits decreasing tendency in the different stages of $\lg\theta$ vs $\lg\varepsilon_p$ for five metallic alloys. Figure 8(b) shows that $\ln\chi_P$ exhibits fluctuant tendency in the deformation stages of $\lg\theta$ vs $\lg\sigma$. This indicates that the sensitivity of work hardening behavior to stress and strain is different. χ_P obtained by full range fitting is close to the lowest value of piecewise fitting, which indicates that full range fitting cannot reflect the complete characteristics of working hardening behaviors.

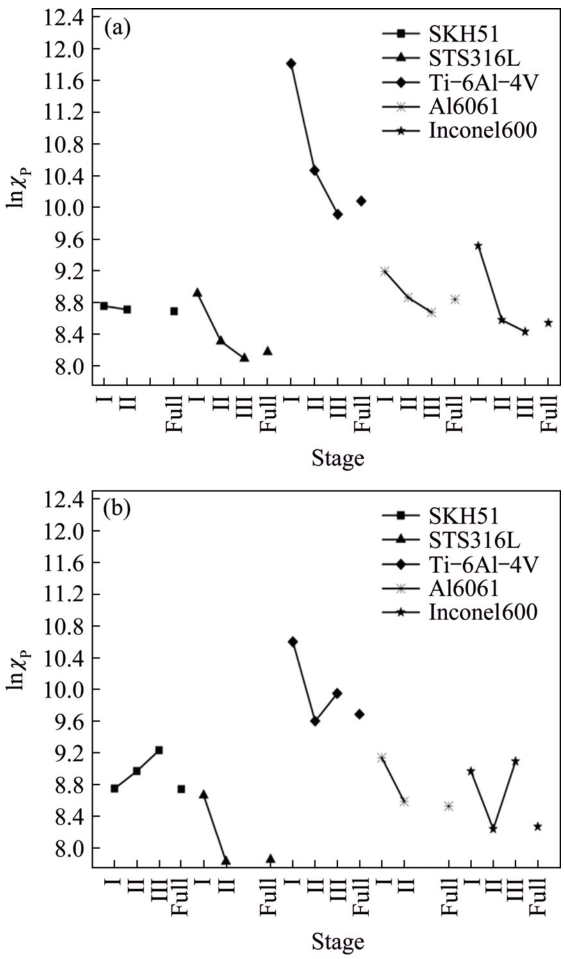

Fig. 8 Comparisons of $\ln\chi_p$ in different stages: (a) $\lg\theta$ vs $\lg\varepsilon_p$; (b) $\lg\theta$ vs $\lg\sigma$

3.3 Yield strengths and ultimate tensile strengths

Figure 9 shows the predicting accuracy of YS and UTS with piecewise and full range fitting by Hollomon, Swift and Voce equations, respectively. For the comparisons between piecewise and full range fitting, piecewise fitting is better than full range fitting to estimate YS with Hollomon equation. In addition, piecewise fitting is almost better than full range fitting to estimate UTS for five metallic alloys, because the entire tensile stress strain behavior contains different strain hardening stages. Therefore, piecewise fitting is better than full range fitting to estimate UTS. In addition, piecewise fitting is meaningful and accurate based on deformation stages in different coordinate transformations.

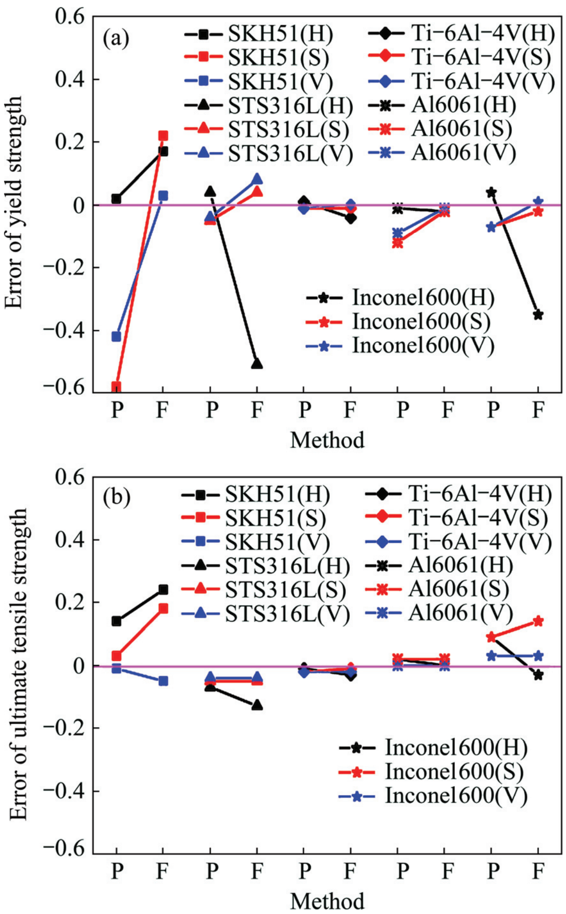

Fig. 9 Predicting accuracy of yield (a) and ultimate tensile (b) strengths using piecewise (P) and full (F) range fitting by three equations for five alloys (H—Hollomon equation; S—Swift equation; V—Voce equation)

For the comparisons of the three typical constitutive equations, Voce equation is the best equation to estimate YS and UTS. Hollomon equation is the worst equation to estimate YS and UTS. The reason is that Hollomon equation itself has unsaturated characteristic of strain hardening and the number of constitutive parameters is less than that of the other equations, while Voce equation has saturated characteristic of strain hardening in large strain region. In addition, Swift and Voce equations start from YS and Hollomon equation starts from 0. That is why the stronger the strain hardening is, the larger the predicting error of YS by Hollomon equation is.

For the comparisons of five metallic alloys, SKH51 is different from the other four metallic alloys to estimate YS and UTS. Its predicting error is larger except for estimating UTS by Voce equation, because the working hardening behavior of SKH51 is different from the other four metallic alloys, as shown in Figs. 2−6.

4 Conclusions

1) The Voce equation is suitable to describe stress−strain curves in large region. Piecewise fitting with original equations is more reasonable than full range fitting to determine constitutive parameters. The constitutive parameters with full range fitting are close to those in the final stages with piecewise fitting.

2) The deformation stages of SKH51 in the three transformations are different from the other four materials. Different working hardening behaviors are found in different coordinate transformations (lg θ vs lg ε_p and lg θ vs lg σ).

3) The predicting accuracy of UTS by using Voce equation is best and the predictive error is about ±5%. Full range fitting is more accurate than piecewise fitting to predict YS with Swift and Voce equations.

References

[1] CHRISTOPHER J, CHOUDHARY B K, SAMUEL E I, MATHEW M D, JAYAKUMAR T. Tensile stress–strain and work hardening behaviour of P9 steel for wrapper application in sodium cooled fast reactors [J]. Journal of Nuclear Materials, 2012, 420(1−3): 583−590.

[2] HOLLOMON J H. Tensile deformation [J]. AIME Trans, 1945, 12(4): 1−22.

[3] VOCE E. The relationship between stress and strain for homogeneous deformation [J]. J Inst Met, 1948, 74: 537−562.

[4] LUDWIGSON D C. Modified stress-strain relation for FCC metals and alloys [J]. Metallurgical Transactions, 1971, 2(10): 2825−2828.

[5] SUNG J H, KIM J H, WAGONER R H. A plastic constitutive equation incorporating strain, strain-rate, and temperature [J]. International Journal of Plasticity, 2010, 26(12): 1746−1771.

[6] FU Zhong-tao, YANG Wen-yu, ZENG Si-qi, GUO Bu-peng, HU Shu-bing. Identification of constitutive model parameters for nickel aluminum bronze in machining [J]. Transactions of Nonferrous Metals Society of China, 2016, 26(4): 1105−1111.

[7] XIAO Gang, YANG Qin-wen, LI Luo-xing. Modeling constitutive relationship of 6013 aluminum alloy during hot plane strain compression based on Kriging method [J]. Transactions of Nonferrous Metals Society of China, 2016, 26(4): 1096−1104.

[8] WEI Guo-bing, PENG Xiao-dong, HU Fa-ping, HADADZADEH A, YANG Yan, XIE Wei-dong, WELLS M A. Deformation behavior and constitutive model for dual-phase Mg−Li alloy at elevated temperatures [J]. Transactions of Nonferrous Metals Society of China, 2016, 26(2): 508−518.

[9] PENG Jian, WANG Yong-jian, ZHONG Li-ping, PENG Long-fei, PAN Fu-sheng. Hot deformation behavior of homogenized Al−3.2Mg−0.4Er aluminum alloy [J]. Transactions of Nonferrous Metals Society of China, 2016, 26(4): 945−955.

[10] CHOUDHARY B K, SAMUEL E I, BHANU S R K, MANNAN S L. Tensile stress–strain and work hardening behaviour of 316LN austenitic stainless steel [J]. Materials Science and Technology, 2001, 17(2): 223−231.

[11] HERTEL S, WAELE W D, DENYS R. A generic stress–strain model for metallic materials with two-stage strain hardening behaviour [J]. International Journal of Non-Linear Mechanics, 2011, 46(3): 519−531.

[12] SAMUEL K G. Limitations of Hollomon and Ludwigson stress–strain relations in assessing the strain hardening parameters [J]. Journal of Physics D: Applied Physics, 2006, 39(1): 203−212.

[13] SAINATH G, CHOUDHARY B K, CHRISTOPHER J, SAMUEL E I, MATHEW M D. Applicability of Voce equation for tensile flow and work hardening behaviour of P92 ferritic steel [J]. International Journal of Pressure Vessels and Piping, 2015, 132−133(S): s1−s9.

[14] KOCKS U F, MECKING H. Physics and phenomenology of strain hardening: The FCC case [J]. Progress in Materials Science, 2003, 48(3): 171−273.

[15] MECKING H, KOCKS U F. Kinetics of flow and strain-hardening [J]. Acta Metallurgica, 1981, 29(11): 1865−1875.

[16] MONTEIRO S N, REED-HILL R E. An empirical analysis of titanium stress-strain curves [J]. Metallurgical Transactions, 1973, 4(4): 1011−1015.

[17] HERTEL S, de WAELE W, DENYS R, VERSTRAETE M. Full-range stress–strain behaviour of contemporary pipeline steels: Part I. Model description [J]. International Journal of Pressure Vessels and Piping, 2012, 92: 34−40.

[18] LECARME L, PARDOEN T. Void growth and coalescence in ductile solids with stage III and stage IV strain hardening [J]. International Journal of Plasticity, 2011, 27(8): 1203−1223.

[19] FARABI N, CHEN D L, ZHOU Y. Tensile properties and work hardening behavior of laser-welded dual-phase steel joints [J]. Journal of Materials Engineering and Performance, 2012, 21(2): 222−230.

[20] SWIFT H W. Plastic instability under plane stress [J]. Journal of the Mechanics and Physics of Solids, 1952, 1(1): 1−18.

[21] KOCKS U F. Laws for work-hardening and low-temperature creep [J]. Journal of Engineering Materials & Technology, 1976, 98(1): 76−85.

[22] KANG S K, KIM Y C, KIM K H, KWON D, KIM J Y. Constitutive equations optimized for determining strengths of metallic alloys [J]. Mechanics of Materials, 2014, 73(1): 51−57.

[23] ZHANG Fan, HUANG Ming-zhi, SHI De-ke. The relationship between the strain-hardening exponent *n* and the microstructure of metals [J]. Materials Science and Engineering A, 1989, 122(2): 211−213.

[24] MEIER M, MUKHERJEE A K. The strain hardening behavior of superplastic Ti−6Al−4V [J]. Scripta Metallurgica et Materialia, 1990, 24(2): 331−336.

[25] RAUCH E F, GRACIO J J, BARLAT F, LOPES A B, FERREIRA DUARTE J. Hardening behavior and structural evolution upon strain reversal of aluminum alloys [J]. Scripta Materialia, 2002, 46(12): 881−886.

[26] ESTRIN Y, TÓTH L S, MOLINARI A, BRÉCHET Y. A dislocation-based model for all hardening stages in large strain deformation [J]. Acta Materialia, 1998, 46(15): 5509−5522.

金属合金的拉伸应力−应变行为

曹 俊，李付国，马新凯，孙占坤

西北工业大学 材料科学与工程学院 凝固技术国家重点实验室，西安 710072

摘　要：利用拉伸应力−应变曲线分析 5 种合金，SKH51、STS316L、Ti−6Al−4V、Al6061 和 Inconel600 的加工硬化行为。通过 Hollomon、Swift 和 Voce 本构模型对材料的实验数据进行拟合、比较与加工硬化特征分析，提出新的预测拉伸变形各阶段加工硬化行为的表征参数及其在不同坐标体系下的表现形式。研究表明，Voce 模型更适合用于描述大应变条件下的拉伸应力−应变关系，其预测抗拉强度的精度高于 Hollomon 和 Swift 模型。另外，SKH51 合金在拉伸变形过程中出现的加工硬化行为明显异于其他 4 种合金。

关键词：本构方程；拉伸应力−应变行为；分段拟合；坐标变换

(Edited by Bing YANG)